CERN - ST Division

THERMAL TRANSIENT ANALYSIS OF TI8 TUNNEL

M. A. Pimenta dos Santos

Abstract

The TI8 tunnel will house a proton beam transfer line of 450 GeV from the SPS to the LHC collider. This line will comprise 340 classical compact design magnets which are expected to dissipate about 120 W/m to the air along the tunnel. As the ventilation injection and extraction points are separated by approximately 2.5 Km (the length of the tunnel), a significant increase in the air bulk temperature is expected along the distance.

This report presents an estimation of the air temperature evolution with time at the end of the tunnel.

1. INTRODUCTION

The TI8 tunnel will house a large number of conventional magnets dissipating heat at a considerable rate during periods of several hours with short pauses in between. Other than the magnets, other heat sources such as cables, water return pipes, lights, etc will generate heat continuously. Starting from fixed ventilation parameters of inlet temperature 17ºC and a flow rate of 22500m^3/h, the calculations presented in this paper seek to estimate the transient air temperature evolution at the end of the tunnel for two different magnet operating cycles.

List of Symbols

$T_{PULSION}$, tunnel inlet air temperature
$T_{EXTRACTION}$, tunnel outlet air temperature
V_{air}, volumetric rate
V_{CV}, moving control volume
h_{CONV}, heat transfer convection coefficient

T_{iw}, inner wall temperature
C_{iw}, inner wall specific heat
ρ_{iw}, inner wall volumetric mass
K_{iw}, inner wall thermal conductivity

T_{ow}, outer wall temperature
C_{ow}, outer wall specific heat
ρ_{ow}, outer wall volumetric mass
K_{ow}, outer wall thermal conductivity

Cp, air specific heat
ρ, air volumetric mass
K, air thermal conductivity

T, air temperature
T_{ROCK}, geothermal fixed temperature

dc, outer wall thickness
diw, inner wall thickness
dr, distance from rock-concrete interface to point of fixed temperature T_{ROCK}.

R_{total}, Conduction resistance from inner wall to point of fixed temperature T_{ROCK}

R, equivalent cylinder radius
P, perimeter of contact air-wall for one tunnel section
r, radial coordinate
z, axial coordinate

w, air average axial velocity
dz, control volume length
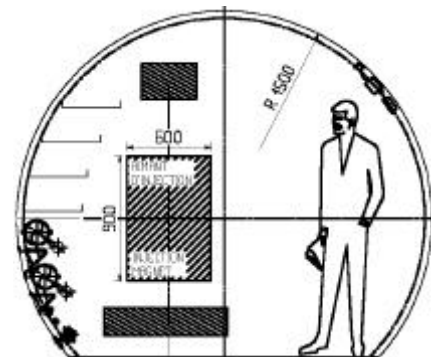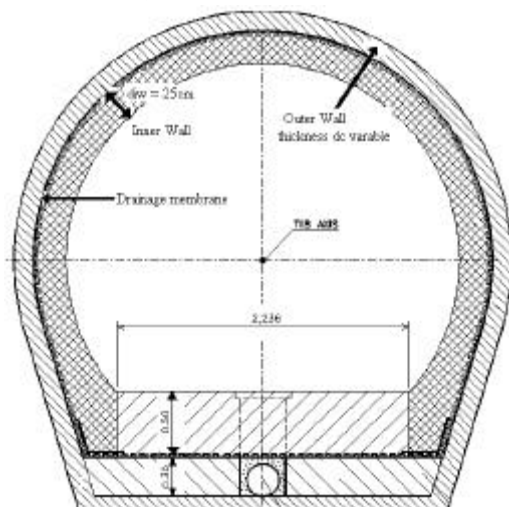
2. PROBLEM DESCRIPTION

2.1 Geometry

Fig.1 – TI8 tunnel wall and interior cross-sectional views

Fig.1 represents a cross-section of the TI8 tunnel. In this report, the mass of concrete interior to the surface defined by the drainage membrane will be referred to as **Inner wall**. Conversely, **Outer wall** will refer to all the mass of concrete exterior to the surface defined by the drainage membrane. As indicated in Fig.1, the outer wall thickness, dc, is variable from point to point thus unknown. The 5cm gap between the two walls contains a 1cm thick plastic drainage membrane and the rest of the volume is filled with air. For the purpose of thermal calculations, this membrane will be ignored and the gap will be assumed as containing only air and referred to as **air gap**.

2.2 Ventilation data and Thermal Loads

Ventilation data:
Volumetric rate, V_{air} = 22500m^3/h = 6.25m^3/s
Area tunnel (free), A=5.55m^2 $\Rightarrow$ air speed, w=1.13m/s
$T_{pulsion}$=17°C

There are four different types of magnets, each one dissipating heat at a different rate as shown in Table 1. Approximately 90% of this heat is assumed to be transferred to the appropriate water cooling circuit incorporated in each magnet, whereas the remaining 10% is assumed to be transferred to the air. The magnets are the only variable heat loads in the tunnel and follow a time history as shown in Fig.2. Constant heat loads include electrical cables, water pipes and other equipment.

Table 1 - Thermal loads[1]

Magnet Type	Power per magnet		Quantity		
MBI	1.1 kW	×	236	=	2596 kW
MQI	2.2 kW	×	86	=	189.2 kW
B340	7 kW	×	12	=	84 kW
B280	8.5 kW	×	6	=	51 kW
				total power	2920.2 kW
		Power loss to the air: 0.1 × total power			**292.01 kW**
				Power/meter	**116.8 W/m**

Constant thermal loads:

Cables	57 kW
Water pipes	11 kW
Others	11 kW
total	**79 kW**
Power/meter	**31.6 W/m**

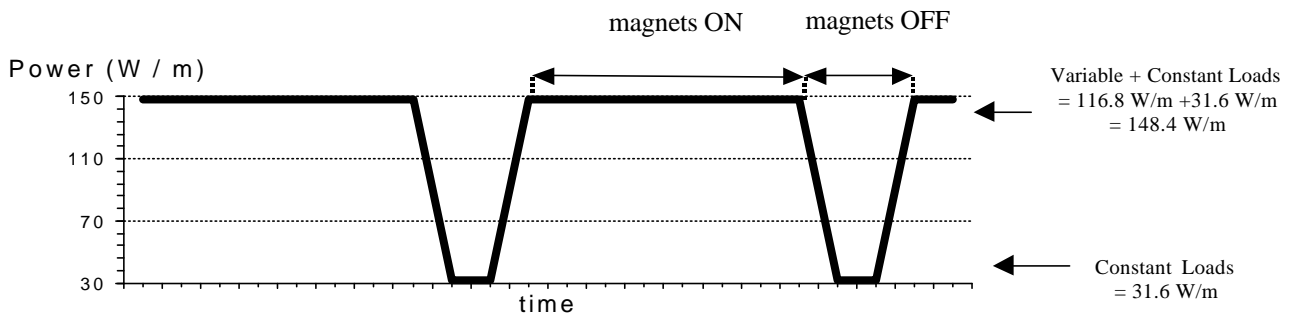1) Data kindly provided by Mr. Volker Mertens from SL/BT Group.

Fig.2 – Heat load time history

In the current paper, calculations will be carried out for three different magnet operating patterns: continuous operation, 6 hours operation followed by a 2 hours pause and 8 hours operation followed by a 2 hours pause.

3. GOVERNING EQUATIONS OF THE THERMAL PROBLEM

The air temperature at the end of the tunnel is highly dependent on the rate of heat transfer to the walls along the distance. In the worst case, if walls were adiabatic the temperature at the end of the tunnel for continuous operation of the magnets would be calculated as follows:

Total power into the air (variable+constant), Q =   292.01+79 kW = 371.02 kW
For air at 40°C (average temperature along the distance), the following properties apply:

ρ = 1.122Kg/m^3
Cp =1004 J/Kg.K

$$T_{EXTRACTION} = T_{PULSION} + \frac{Q}{\rho \cdot V_{air} \cdot Cp} \quad T_{EXTRACTION} \approx 69.5°C$$

To render the problem computationally affordable, some simplifications must be made. The first is to consider an equivalent cylindrical tunnel having the same free and wall cross-sectional area as the real tunnel, as shown in Fig.3. The radius R of such a cylinder is calculated in appendix I. The area of contact wall-air for convective heat transfer purposes remains the same as in the real tunnel.
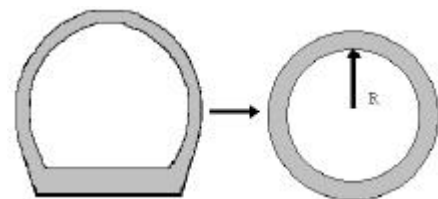

Fig.3 – TI8 tunnel and equivalent cylinder having the same free and concrete area

4

Another important simplification is to assume uniform air temperature at a given cross-section and moment in time i.e. to consider the flow as being 1-Dimensional. Under these hypotheses, a heat balance can be written for a control volume V_{CV} of air moving along with the flow at speed w (see Fig.4):

$$\left(\rho_{(z,t)} \cdot V_{CV} \cdot Cp_{(z,t)}\right)\left(\frac{\partial T_{(z,t)}}{\partial t} + w\frac{\partial T_{(z,t)}}{\partial z}\right) = \dot{q}_{E(t)} \cdot dz - P \cdot dz \cdot h_{CONV}\left(T_{(z,t)} - T_{W\,(r=R,z,t)}\right) \quad (\,1\,)$$

where

R is the equivalent cylinder radius

P.dz is the area of contact air-wall (see Appendix I)

$P \cdot dz \cdot h_{CONV}\left(T_{(z,t)} - T_{W(r=R,z,t)}\right)$ is the heat transferred to the wall by convection

$q_{E(t)}$ is the heat dissipated per meter by the equipment (magnets, cables, etc)

V_{cv} , the moving control volume is given by $V_{cv} = 2\pi R.dz$

$\frac{\partial T}{\partial t} + w\frac{\partial T}{\partial z}$ is known as the substantial derivative and accounts for the fact that the

control volume follows the flow, i.e., T=T(z,t) $\Rightarrow \frac{dT}{dt} = \frac{\partial T}{\partial t} + w\frac{\partial T}{\partial z}$
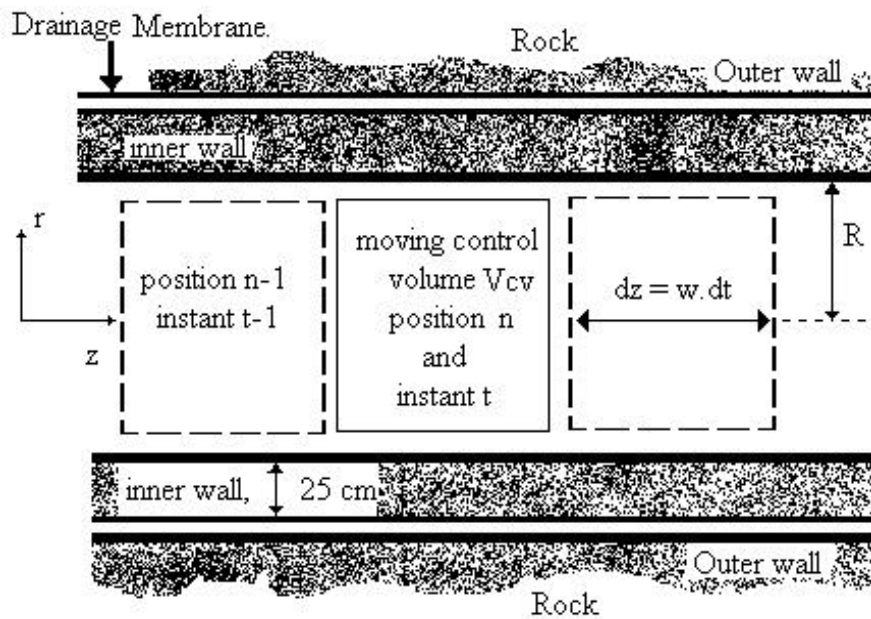

Fig.4 – Moving control volume considered for the heat balance

The temperature in the wall is a function of r, z and t and obeys the following equation (in cylindrical coordinates and symmetry with respect to the axis):

$$\frac{\partial}{\partial r}\left(K_{W(r)}\frac{\partial T_{W(r,z,t)}}{\partial r}\right)+\frac{K_{W(r)}}{r}\cdot\frac{\partial T_{W(r,z,t)}}{\partial r}+K_{W(r)}\frac{\partial^2 T_{W(r,z,t)}}{\partial z^2}=\rho_{W(r)}C_{W(r)}\cdot\frac{\partial T_{W(r,z,t)}}{\partial t}\qquad(\,2\,)$$

and the coupling between wall and air temperature being given by:

$$h_{CONV}\left(T_{(z,t)}-T_{W(r=R,z,t)}\right)=-K_W(r)\frac{\partial T_W}{\partial r}\bigg|_{r=R}\qquad(\,3\,)$$

3.1 Some justified simplifications

Although equation (2) is the exact description of the temperature evolution in the wall, it complicates considerably the solution of the whole system of equations (1), (2) and (3). However, the problem can be simplified significantly if the following hypotheses are made:

i)   Conduction resistance is ignored for the inner wall, i.e. the temperature is considered uniform at any given instant for R′r′R+ diw

ii)   Temperature is fixed to the geothermal temperature (Trock) at a certain point in the rock (see Fig.5)

iii)   Thermal heat capacity is ignored for the outer wall and for the rock.

iv)   Conduction along z is neglected

The type of simplification made in (i) is called the lumped-heat-capacity method. Such system is obviously idealized because a temperature gradient must exist in the concrete if heat is to be conducted into or out of the inner wall. The assumption of uniform temperature distribution throughout each cross-section of the inner wall is equivalent to saying that the surface-convection and air gap resistance are large compared with the internal-conduction resistance as shown below:

Internal- conduction resistance per meter length
of equivalent cylinder is:

$$Riw=\frac{\ln\left(\dfrac{R+diw}{R}\right)}{2\pi\cdot K_{iW}}=\frac{\ln\left(\dfrac{1.329+0.32}{1.329}\right)}{2\pi\cdot 1.37}=0.025K/W\,m$$

Air gap resistance per meter of length of
equivalent cylinder is:

$$Rag=\frac{\ln\left(\dfrac{R+diw+0.05}{R+diw}\right)}{2\pi\cdot K}=\frac{\ln\left(\dfrac{1.329+0.32+0.05}{1.329+0.32}\right)}{2\pi\cdot 0.02624}=0.182K/W\,m$$

Convection resistance per meter of length of tunnel (see Appendix II)

$$0.020\ K/\ W.m\le\qquad R_{CONV}\quad=\frac{1}{P\cdot h_{CONV}}\qquad\le 0.06\ K/\ W.m$$

so Riw compared witht Rag+Rconv is:

$$0.1 \leq \frac{R_{iw}}{R_{ag} + R_{CONV}} \leq 0.12$$

Simplification (ii) is equivalent to assuming that at a certain distance from the outer wall, the mass of rock is large enough to absorb heat without having its temperature increased in the process.

Simplification (iii) stems from (ii) and means that none of the heat conducted from the inner wall through the air gap is absorbed and used to raise the temperature of the outer wall and rock.

Conduction along z can be neglected since wall temperature gradients in this direction are very small. Fig. 5 shows the simplified thermal model and the equivalent electrical circuit.
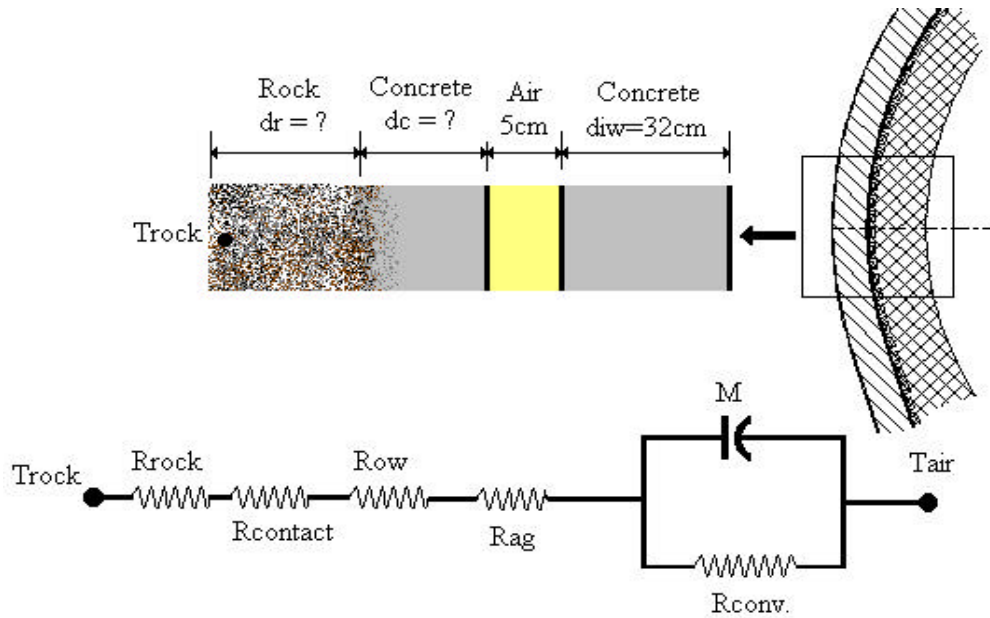

Fig.5 – Simplified thermal model and equivalent electrical circuit

With the simplifications introduced above, equation (2) and (3) are replaced by:

$$C_{iw} \cdot \rho_{iw} \cdot V_{iw} \cdot \frac{\partial T_{iw}}{\partial t} = P \cdot dz \cdot h_{CONV}(T_{(z,t)} - T_{iw(z,t)}) - \frac{T_{iw(z,t)} - T_{ROCK}}{R_{total}} \qquad (4)$$

3.2 Discretization of the Governing Equations

Equations (1) and (4) can now be discretised using the following approximations

$$\frac{\partial T_{(z,t)}}{\partial t} \approx \frac{T_t^n - T_{t-1}^n}{\Delta t} \qquad \textbf{(5a)}$$

$$\frac{\partial T_{(z,t)}}{\partial z} \approx \frac{T_t^n - T_t^{n-1}}{\Delta z} \qquad \textbf{(5b)}$$

$$T_{(z,t)} - T_{iw(r=R,z,t)} \approx T_{t-1}^{n-1} - T_{iw\,t-1}^{n} \qquad \textbf{(5c)}$$

$$\frac{\partial T_{iw}}{\partial t} \approx \frac{T_{iw\,t}^{n} - T_{iw\,t-1}^{n}}{\Delta t} \qquad \textbf{(5d)}$$

to become, after some rearrangements,

$$T_t^n = \frac{1}{2}\left[T_{t-1}^n + T_t^{n-1} - \frac{2\Delta t}{Cp \cdot \rho \cdot R} \cdot h_{CONV}\left(T_{t-1}^{n-1} - T_{iw\,t-1}^{n} \right) + \frac{\Delta t \cdot q_E}{Cp \cdot \rho \cdot \pi R^2} \right] \qquad \textbf{(6)}$$

and

$$T_{iw\,t}^{n} = \frac{2\pi R \cdot w \cdot \Delta t^2}{C_{iw} \cdot \rho_{iw} \cdot V_{iw}} h_{CONV}\left(T_{t-1}^{n-1} - T_{iw\,t-1}^{n} \right) - \frac{\Delta t}{C_{iw}\,\rho_w V_w R_{total}}\left(T_{iw\,t-1}^{n} - Trock \right) + T_{iw\,t-1}^{n} \qquad \textbf{(7)}$$

A computer code in FORTRAN77 was written to solve this system of equations. As justified in Appendix III, R_{total} ranges from 0.0093 K/W to 0.013 K/W. Likewise, as justified in Appendix II, h_{conv} ranges from 1.8 W/K.m^2 to 5.4 W/K.m^2. Taking into account the geothermal gradient, the rock temperature Trock, at the TI8 tunnel average depth (75 m), is in the vicinity of 12ºC. It is also shown in Appendix IV that with a control volume length of dz = 25m, convergence of solution is secured.

4. RESULTS

4.1 Case 1: Magnets Operating Continuously

Fig.6 and Fig.7 represent air temperature evolution at the end of the TI8 tunnel for the two extreme values of h_{CONV}. It can be seen that temperature reaches 22°C to 29°C in after one day and stabilises between 40.5°C and 47°C after 23 to 26 days. It can also be noticed that in the short term h_{conv} is the major influence on the temperature variability whereas the influence of R_{total} becomes important only in the short to long term.
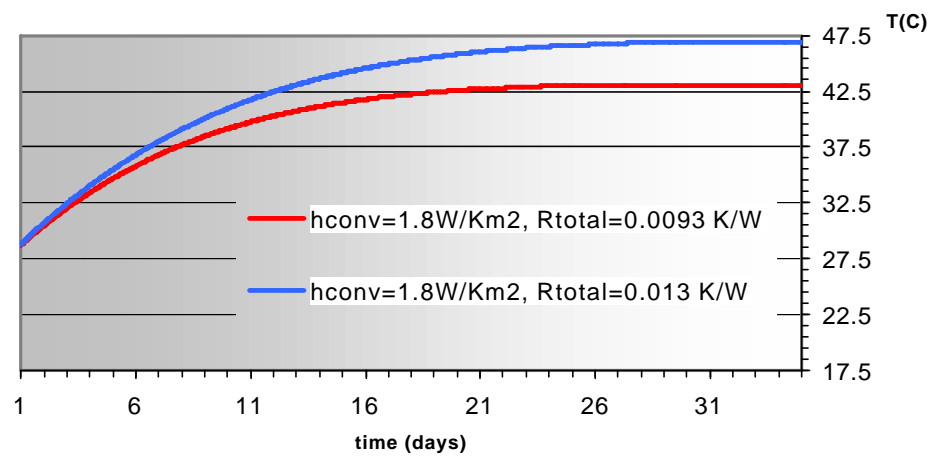
Fig. 6 – Air temperature evolution at the end of tunnel TI8 for magnets operating without interruption and h_{CONV}=1.8 W/Km^2
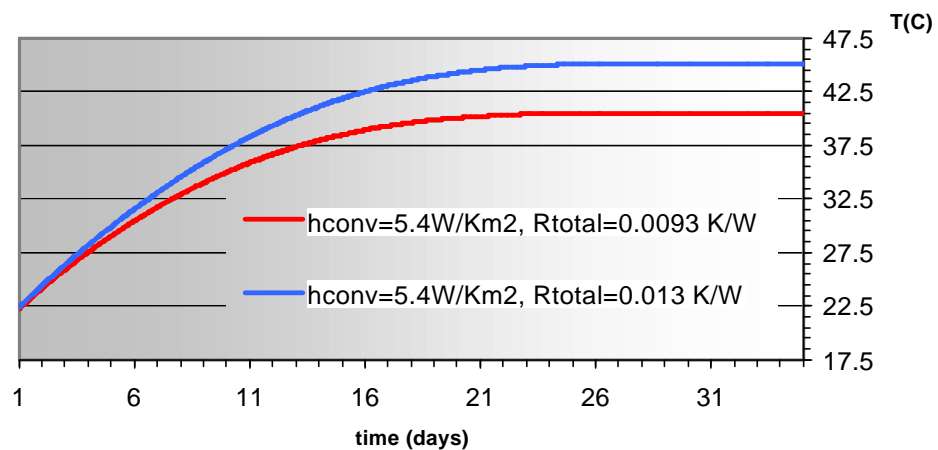
Fig. 7 – Air temperature evolution at the end of tunnel TI8 for magnets operating without interruption and h_{CONV}=5.4 W/Km^2

4.2 Case 2: Operation Cycle 8h ON + 2h OFF

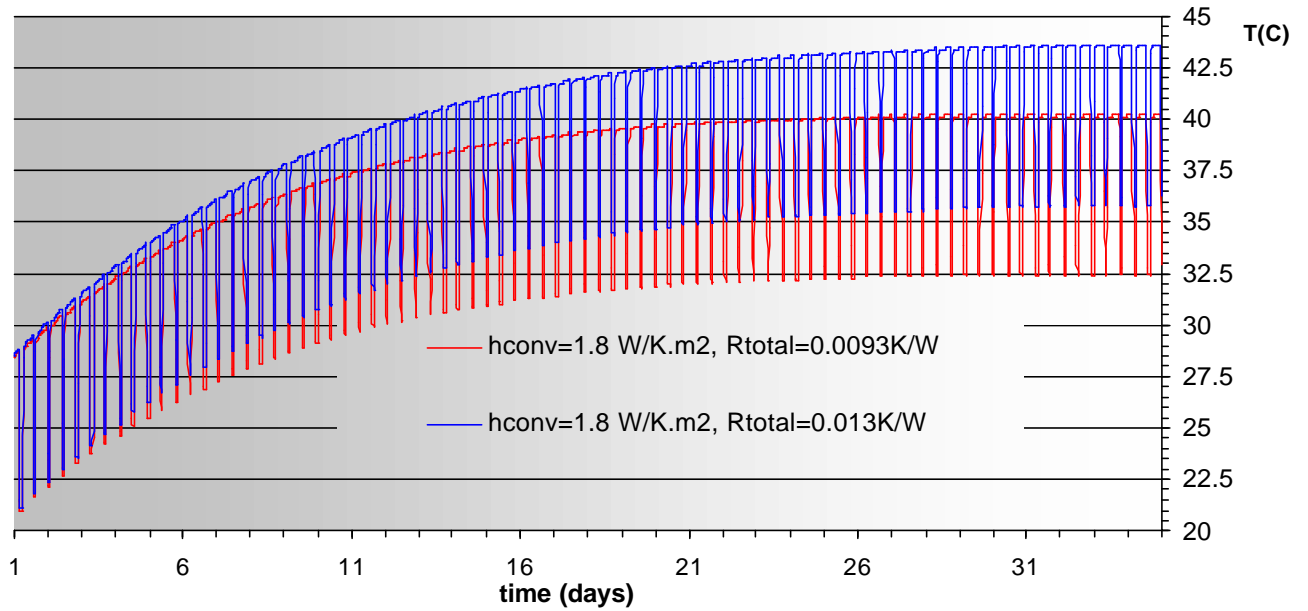**Fig. 8** – Air temperature evolution at the end of the tunnel for a cycle 8h + 2h
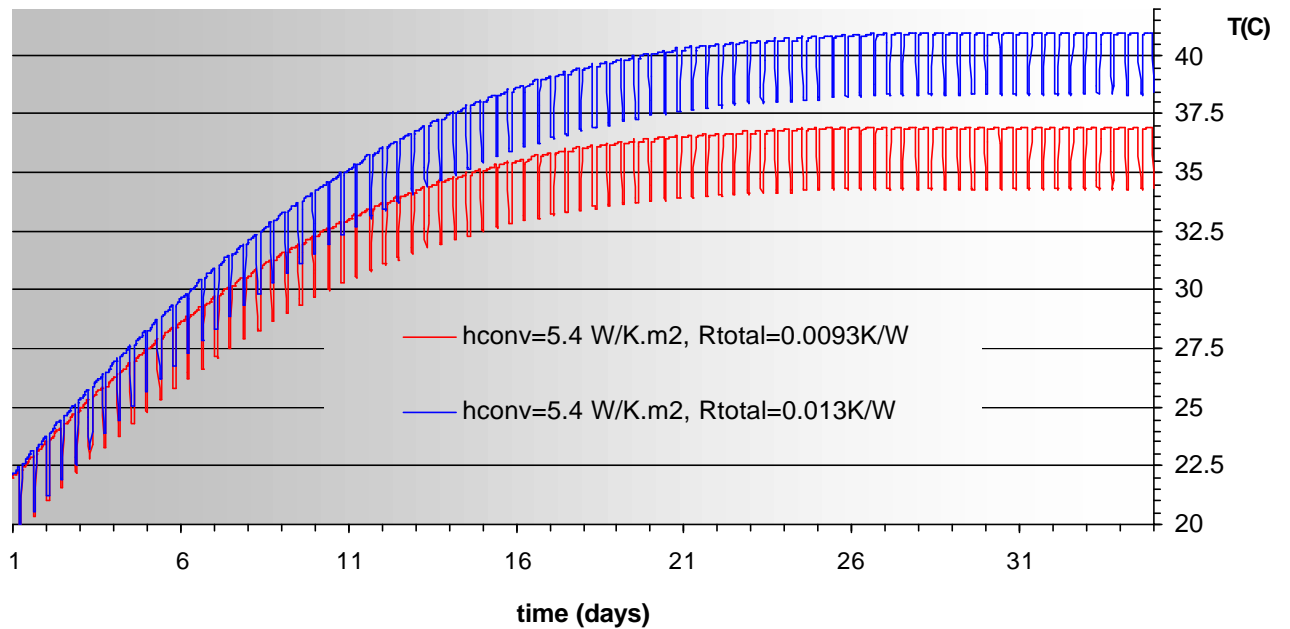and $h_{conv} = 1.8 \ W/K.m^2$

Fig. 9 – Air temperature evolution at the end of the tunnel for a cycle 8h + 2h
and $h_{conv} = 5.4 \ W/K.m^2$
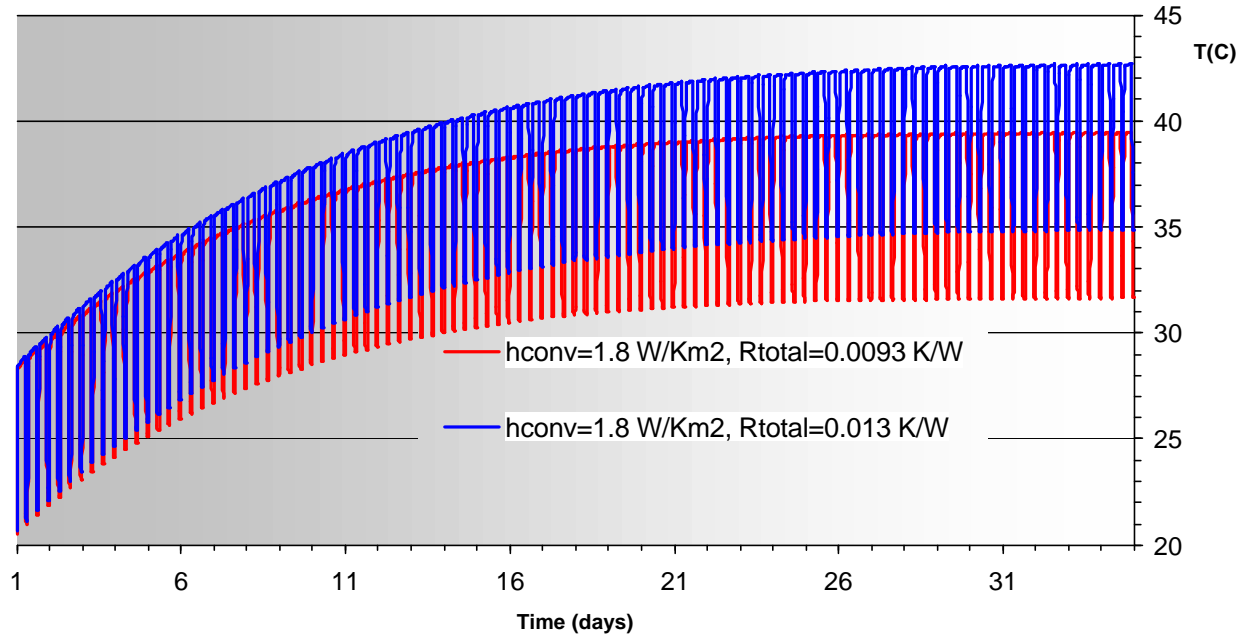
4.3 Case 3: Operation Cycle 6h ON + 2h OFF

Fig. 10 – Air temperature evolution at the end of the tunnel for a cycle 6h +2h
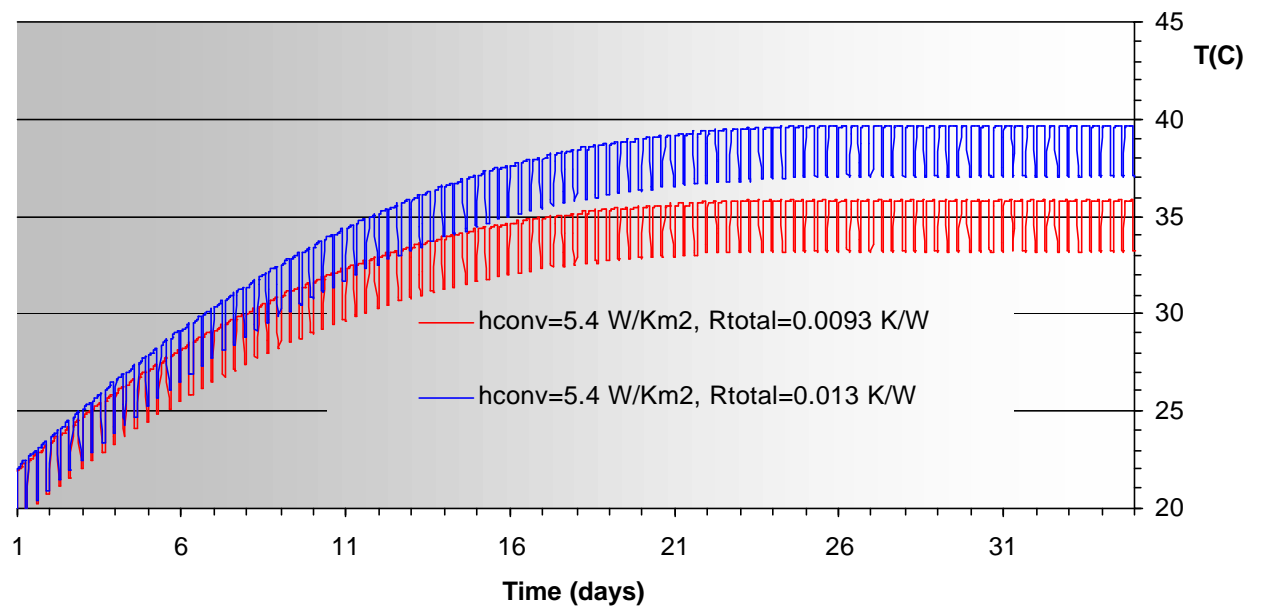and $h_{conv} = 1.8$ W/K.m^2

Fig. 11 – Air temperature evolution at the end of the tunnel for for a cycle 6h +2h
and $h_{conv} = 5.4$ W/K.m^2

5. SUMMARY OF RESULTS

Table 2 summarises results from Fig.6 to 11. It can be seen that the uncertainties in the wall thermal behaviour as well as in the air-wall heat transfer coefficient lead to wide limits for the expected temperature in the tunnel. Nevertheless, the calculations show that pauses of two hours cause only a reduction of about 4°C from the steady state temperature reached with continuous operation. Moreover, when shortening the time ' ON ' from 8h to 6h, the temperature drop achieved in the steady state is merely 1°C.

Table 2 – Summary of estimated limits for temperature at the end of TI8 tunnel

Magnets' Operating Pattern	Temperature after 1 day	Stabilised Temperature
Case 1: Continuous Operation	22°C≤T≤29°C	40.5°C≤T≤47°C reached after 22 to 28 days
Case 2: 8h ON + 2h OFF	22°C≤T≤28.5°C	When Magnets are ON 37°C≤T≤43.6°C When Magnets are OFF 32.5°C≤T≤38.5°C reached after 25 to 30 days
Case 3: 6h ON + 2h OFF	22°C≤T≤28.5°C	When Magnets are ON 35.9°C≤T≤42.7°C When Magnets are OFF 31.8°C≤T≤37°C reached after 25 to 30 days

It also stands out from the same plots that an increase in the convection heat transfer coefficient reduces the amplitude of temperature variation between periods ON and OFF. This can be explained by the fact that when magnets are ON, heat is transferred from the air into the walls whereas when magnets are OFF part of this heat is returned back to the air. A higher heat transfer coefficient means more heat being returned to the air during the period OFF and thus a smaller drop in air temperature from the preceding period ON.

Only the temperatures at the tunnel outlet were presented in this report. The corresponding values for any other point at any instant can be obtained by with good approximation by interpolating linearly between the inlet and outlet temperatures for that same instant.

6. CONCLUSIONS

For an inlet temperature of 17°C and volumetric rate 22500m^3/h, air temperatures at the end of TI8 tunnel are expected to range between 22°C and 29°C after 24 hours of operation. For cycles of 6 to 8 hours of magnet operation followed by 2 hours pauses, the air temperature is expected to stabilise between 36°C and 44°C after a transient monotone evolution of 25 to 30 days.

If magnets are operated without pauses, temperature at the end of the tunnel stabilises between 41°C and 47°C after 22 to 28 days.

7. ACKNOWLEDGEMENT

APPENDIX I - Calculation of equivalent cylinder

TI8 Tunnel area = 6.27 m^2

TI8 Tunnel free area:
(blue area on Fig. AI.1) = 5.55 m^2

Inner wall area :
(red area + green area on Fig. AI.2) $\approx$ 2.99 m^2

Equivalent cylinder radius: $R = \sqrt{\dfrac{5.55}{\pi}} = 1.329 m$

Fig. AI.1

The equivalent cylinder inner wall thickness, diw, is calculated to maintain the same volume of concrete:

$$\pi\left[(R + diw)^2 - R^2\right] = 2.99 m^2 \rightarrow \text{diw} = 0.32\text{m}$$

Note: the inner wall thickness for the real tunnel varies from 0.25m (red area) to 0.5m (green area).

For convection heat transfer calculation purposes, the area used was that of the real tunnel, i.e. P.dz where P is the wall exposed perimeter

$$P = 2.236 + 2\pi \times 1.5 \times \frac{(2w + 180)}{360} = 9.15 m$$

with w $\approx$ 42°

Fig. AI.2

Note: the exposed perimeter for the equivalent cylinder is 8.35m
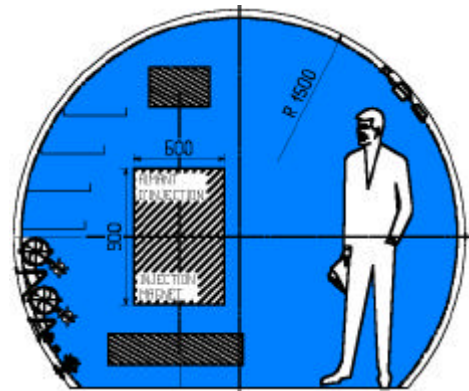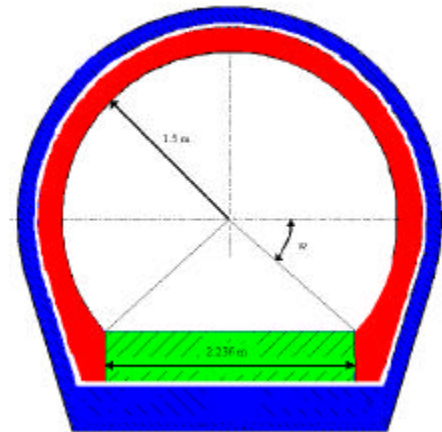
APPENDIX II - Calculation of h_{conv}

Calculations are based on the equivalent cylindrical tunnel defined in **APPENDIX I**

Reynolds number: Prandtl number for air at 300K:

$$Re = \frac{w.2.R}{\upsilon_{air}} = \frac{1.13 \times 2 \times 1.329}{1.5 \times 10^{-5}} = 2.002 \times 10^5 \qquad Pr = 0.707$$

For fully developed turbulent flow, convection heat transfer can be calculated by the expression recommended for smooth pipes by Dittus and Boelter[1]:

$$h_{conv} = \frac{k}{2 \cdot R} \cdot 0.023 \, Re^{0.8} \, Pr^{0.3}$$

$$h_{conv} = \frac{0.02624}{2 \cdot 1.329} \cdot 0.023 \cdot (2.002 \times 10^5)^{0.8} (0.707)^{0.3} = 3.57 \, W\!\!\Big/\!\!{K \cdot m^2}$$

However, the assumption of smooth pipe is somehow idealistic, as the tunnel is partially obstructed with equipment (see Fig.1) and is not cylindrical. This modifies considerably the velocity profile and introduces uncertainty on the value of h_{conv} however it is reasonable to assume an error margin of 50%, i.e.

$$1.8 \text{ W/K.m}^2 \leq h_{conv} \leq 5.4 \text{ W/K.m}^2$$

---

1) Dittus, F.W., and L.M.K. Boelter: Univ. Calif. (Berkeley) Pub. Eng.,vol.2, p.443,1930.

APPENDIX III – Variability of R_{total}

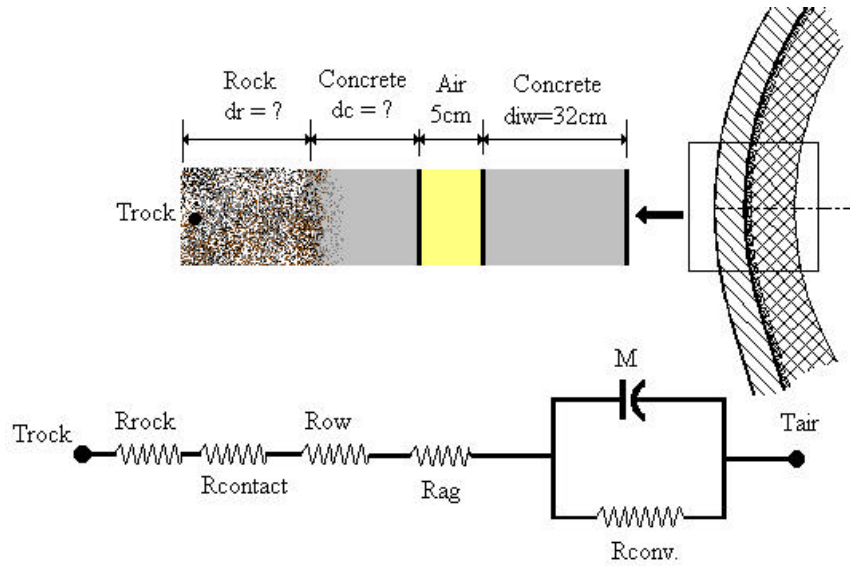**Fig. AIII-1** – Simplified Thermal model and equivalent electrical circuit

The total conduction resistance is R_{total} = Rag + Row + Rcontact+ Rrock and is given, for a tunnel segment of length dz, by the formulae below. Note that R=1.329 m and diw=0.32 m as calculated in appendix I. The outer wall thermal conductivity, K_{ow} = K_{iw} =1.37 W/m.K   (conductivity of concrete obtained from   Holman J.P., 1997, *Heat Transfer*, McGraw-Hill, New York). The inner wall thermal capacity is given by M=ρ_{iw} 3 C_{iw} 3$\pi\{(R+diw)^2 - R^2)\}$.dz .

Table 3 - Components of R_{total}

$Rag = \dfrac{\ln\left(\dfrac{R+diw+0.05}{R+diw}\right)}{2\pi \cdot K \cdot dz}$	Air gap conduction resistance
$Row = \dfrac{\ln\left(\dfrac{R+diw+0.05+dc}{R+diw+0.05}\right)}{2\pi \cdot K_{OW} \cdot dz}$	Outer wall conduction resistance
$Rcontact = \dfrac{\ln\left(\dfrac{R+diw+0.05+dc+0.01}{R+diw+0.05+dc}\right)}{2\pi \cdot K \cdot dz}$	Contact resistance between the outer wall and the rock was assumed as being equivalent to 1cm of air
$Rrock = \dfrac{\ln\left(\dfrac{R+diw+0.05+0.01+dc+dr}{R+diw+0.05+0.01+dc}\right)}{2\pi \cdot K_{ROCK} \cdot dz}$	Rock conduction resistance to the point where temperature is fixed at Trock

The outer wall thickness dc, the length dr of rock to the point of fixed temperature Trock and the rock conductivity K_{rock} are needed to calculate R_{total}. The two former

parameters vary from point to point yet it is reasonable to assume the following limits for their variation:

$$0.1m < dc < 0.5m \qquad 0.5m < dr < 5.0m$$

The type of rock found at the typical depth of CERN tunnels is known as 'green sandstone' ('molasse' in French) and is a mixture of sedimentary rock of compressed sand and marl (mixture of clay and lime). Table 4 shows the thermal conductivity values for this particular green sandstone, obtained from O. Johansen : *Thermal Conductivity of soils*. Ph.D. Thesis – Trondheim 1975.

Table 4 – Thermal conductivity for each component of green sandstone

type	Conductivity (W/ m. K)	% in Geneva's green sandstone
sandstone	3.560.9	45
marl sandstone	3.060.8	26
marl	2.660.7	29
weighted average	3.160.8	100

Thus, the value of K_{rock} will be considered to vary in the interval

$$2.3 \; W/m.K < K_{rock} < 3.9 \; W/m.K$$

Rtotal for Krock = 2.3 W/m.K

	dc = 0.1m	dc = 0.5m
dr = 0.5m	**0.0096**	0.01
dr = 5.0m	0.013	**0.013**

Rtotal   for Krock = 3.9 W/m.K

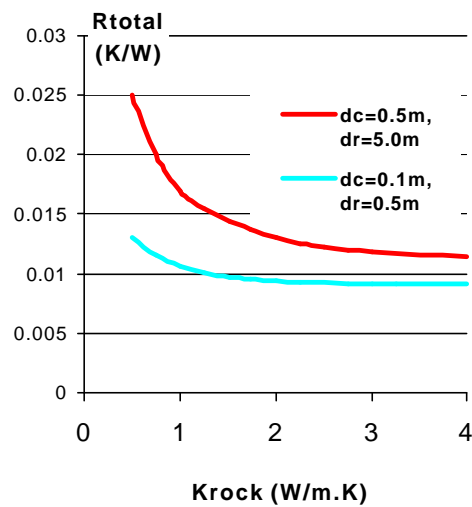|	dc = 0.1m	dc = 0.5m
dr = 0.5m	**0.0093**	0.0099
dr = 5.0m	0.011	**0.011**

Fig. AIII-2 – Dependence of R_{total} on the value of K_{rock} for extreme values of dc and dr

So calculations will be done for

Rtotal= 0.0093 K / W and 0.013 K / W to cover the whole range of values